Numerical Simulations of Spherical Gap Flows

K. Buehler*, J.W. Louw
University of Applied Sciences Offenburg,
*Corresponding author: Badstrasse 24, D 77652 Offenburg; Email: k.buehler@fh-offenburg.de

Dedicated to Professor Dr.-Ing., Dr.h.c.
O. Felsch on the occasion of his 80. birthday

Abstract: Rotating fluids are important in nature and technology. Many applications can be found in the field of meteorology and in rotating machinerys. This investigation concern the application of swirl flow mode of COMSOL MULTIPHYSICS to simulate nonlinear aspects of flows within spherical geometries. The results show the non-uniqueness of the supercritical solutions and interesting aspects of the connected bifurcations. Symmetric and asymmetric solutions and transient bifurcations are realized in the supercritical Reynolds number regime. A comparison of the results from the numerical simulations with the experiments in spherical gap flows shows a good agreement concerning the flow structure, bifurcations and existence ranges.

Keywords: Spherical gap flow, rotating fluids, bifurcation, non-uniqueness, Taylor vortices

1. Introduction

The swirl flow code of COMSOL MULTIPHYSICS is used to simulate the flow between two concentric spheres. The flow is induced by the rotation of the inner sphere about their vertical axes. A comprehensive investigation of the flow between two concentric spheres is reported by Sawatzki and Zierep [1] , Wimmer [2] and Bühler [3]. A principal sketch of the spherical gap geometry is shown in Figure 1. The flow is described with cylindrical coordinates, that means r in radial direction with velocity component u and z in axial direction with velocity component v. In circumferential direction φ acts the velocity component w. The flow is restricted to rotationally symmetric flow structures and therefore all velocity components are independent of the circumferential coordinate φ. The fluid is contained between the two concentric spherical boundaries. The flow can be realized by the rotation of the inner sphere and by superimposing a throughflow in meridional direction. In this investigation the throughflow in meridional direction is zero. The basic flow is always three-dimensional. In spherical gaps no simple basic flow like the one-dimensional Couette flow between two concentric rotating cylinders exist. The bifurcation scenario for closed gaps is described in a review article by Bühler[4]. In this investigation we explore new bifurcation scenarios to explane the supercritical flow behaviour. The finite element method is useful to confirm the former results obtained with a finite difference method and to entend the informations of the pattern formation connected with multiple solutions in the nonlinear domain of high Reynolds numbers.

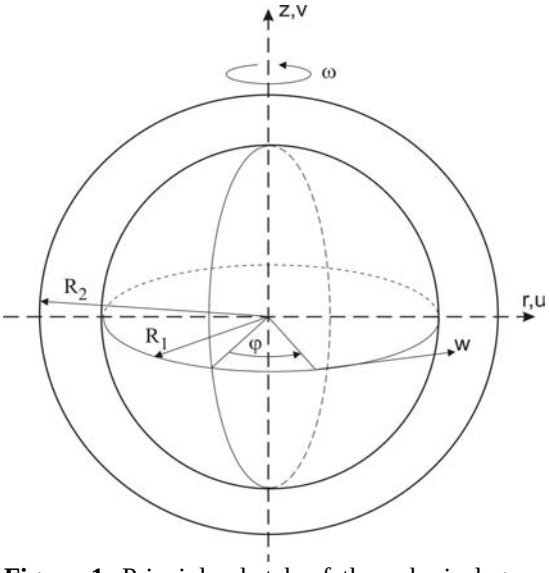

Figure 1. Principle sketch of the spherical gap geometry, cylindrical coordinates and velocity components

2. Simulations with COMSOL Multiphysics

The swirl flow module of COMSOL MULTIPHYSICS enables the calculations of flows within geometries defined in cylindrical coordinates. In this paper it is shown, that this module can be applied to address rotational symmetric flows within spherical boundaries. The initial and boundary conditions are the same

as in the experiments. The fluid properties are incompressible and Newtonian.
The results are visualized with lines of constant stream function in the meridional plane. The poisson equation is used to calculate the stream function based on the velocity components which results from the numerical simulations. The steady states are reached after time-dependent calculations up to the final steady state. The torque acting by the fluid on the inner sphere is calculated and compared with experimental results.

3. Results of numerical simulations

The supercritical flow exhibits clearly the non-uniqueness of the Navier-Stokes equations. Depending on the initial conditions, the supercritical solutions can be separated by different accelerations. Special transitions between the supercritical solutions are described.
The three supercritical modes of flow have different numbers of vortices near the equatorial region.
The supercritical flow Mode I (Figure 2 a) without vortices is realized by a sudden acceleration from subcritical to supercritical Reynolds number. The Mode IV (Figure 2 c) with four vortices occur after slowly acceleration of the inner sphere. The Mode III (Figure 2 b) with two vortices needs a asymmetric transition with respect to the equatorial symmetry plane.
A new bifurcation szenario is given in Figure 3. Starting with different Reynolds numbers from rest we get the different rotationally symmetric modes depending on time. The existence ranges of the modes with and without vortices are shown as function on Reynolds number and time. Below the Reynolds number Re=800 the basic flow exists as subcritical Mode I without vortices. In the range of Reynolds numbers between Re=800 and Re=890 the Mode III with two vortices near the equator occurs after a asymmetric transition (Mode III_B) with respect to the equator. For higher Reynolds numbers up to Re=1700 we find the symmetric Mode IV with four vortices near the equator. In the Reynolds number range between Re=1700 and Re=1930 we obtain the asymmetric Mode III_A with two vortices asymmetric with respect to the equator as final steady state. This new bifurcation was not known from the simulations with a finite difference method described in [4].

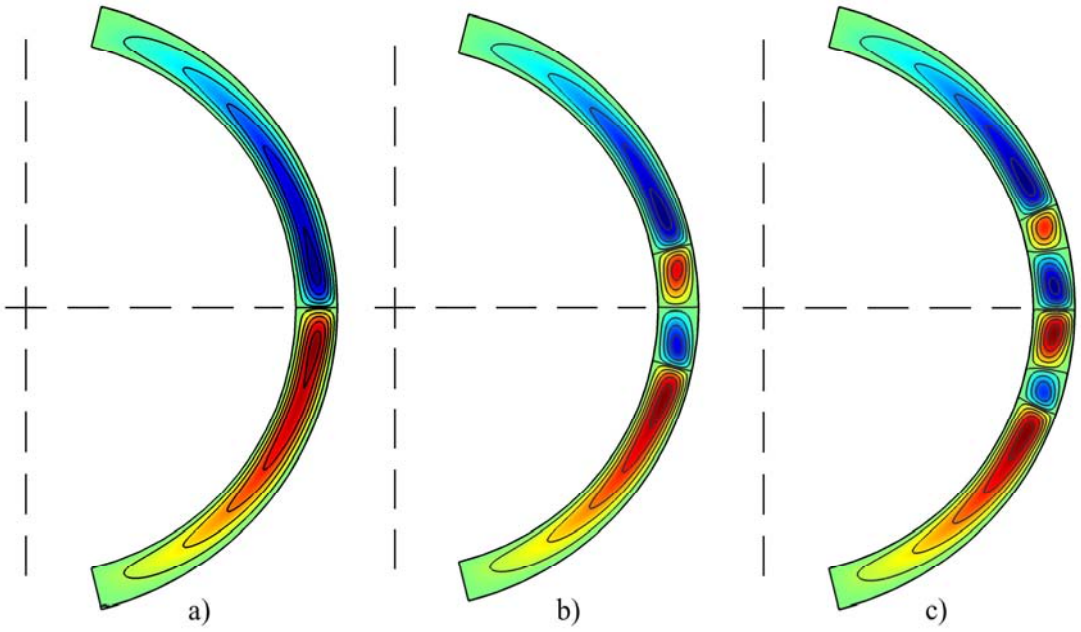

Figure 2. Non-uniqueness of supercritical solutions in spherical gap flow, a) Mode I without vortices, b) Mode III with two vortices , c) Mode IV with four vortices near the equator
R_1= 65 mm, R_2= 75 mm, $\sigma = (R_2 - R_1)/R_1 = 0.154$, $Re = R_1^{2} \cdot \omega^2/\nu = 2600$

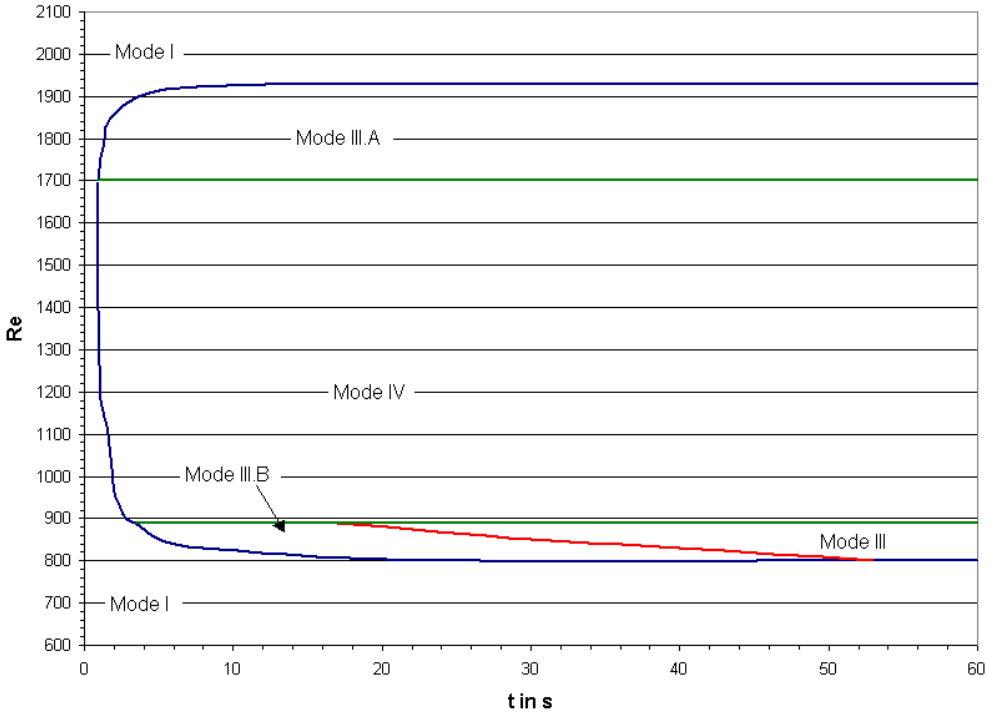

Figure 3. Existence ranges after sudden start from rest for the different modes depending on the time t

It is very interesting, that only the two vortex mode can occur as asymmetric steady state with respect to the equator. For Reynolds numbers higher than Re=1930 the supercritical Mode I without vortices occurs after the sudden start of the inner sphere to the final Reynolds

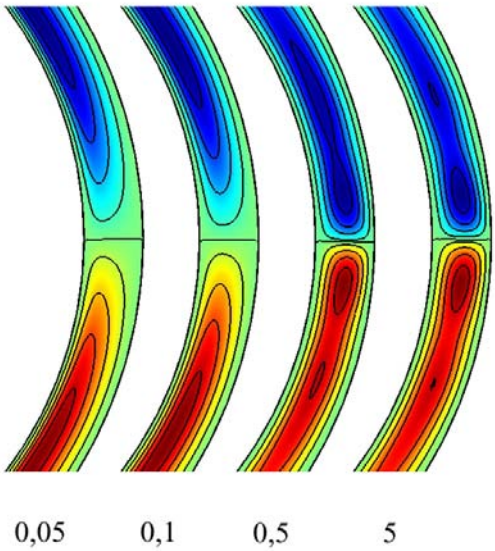

Figure 4. Symmetric transition from rest into supercritical Mode I at Re=2000

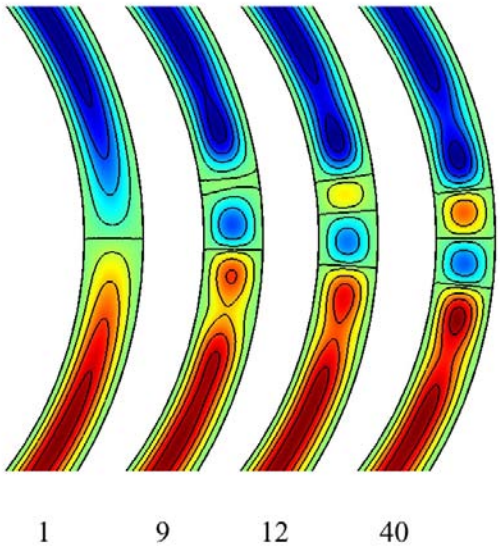

Figure 5. Asymmetric transition from rest into supercritical Mode III at Re=830

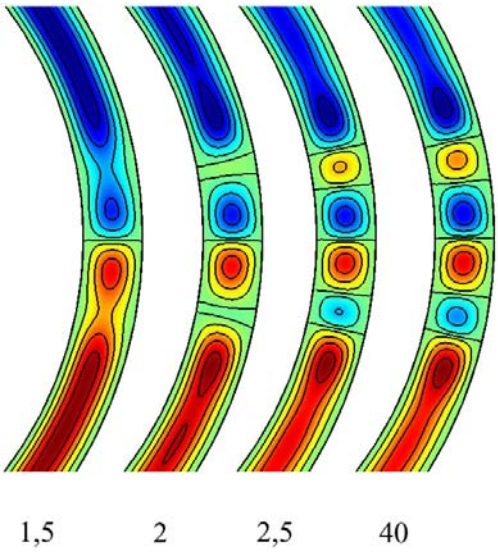

Figure 6. Symmetric transition from rest into supercritical Mode IV at Re=1000

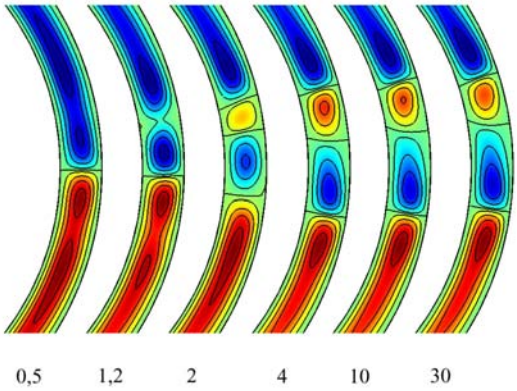

Figure 7. Asymmetric transition from rest into supercritical Mode III_A at Re=1800

number.The flow structures during the time-dependent development of the different modes are shown in the following Figures. The sudden start from rest to a Reynolds number Re=2000 leads to the supercritical flow without vortices called Mode I. Figure 4 shows the flow structure visualized with lines of constant streamfunction. The intensification of the flow in the meridional plane with increasing time is clearly displayed. The final state is connected with a strong flow in radial direction in the equatorial plane.

The transition from the basic state into the two vortex state Mode III at Re=830 occurs asymmetric with respect to the equator as shown in Figure 5. This behaviour is necessary to change the flow direction in the equatorial plane from the direction outwards during the basic flow into the direction radially inward for the two vortex flow. Starting from rest to a Reynolds number Re=1000 we get the symmetric transition from the basic flow into the four vortex state Mode IV. This transition shown in Figure 6 develops symmetrically with respect to the equator. The vortices directed with the basic flow are more intensive compared with that vortices moving in opposite direction. The reason for this symmetric transition is the fact, that the flow direction in the equatorial plane is the same during the full transition.

The transition into the final asymmetric state Mode III_A is shown in Figure 7 for the Reynolds number Re=1800. The vortices are developed in the upper hemisphere and move then towards the lower hemisphere into the final steady state. This Mode III_A is a very interesting state, since he consists of a asymmetric flow connected with symmetric boundary conditions of the spherical gap.

The torque behaviour during the transitions into the different modes of flow are shown in Figure 8 as function of time. The asymmetric transition into the Mode III needs the most time to reach the steady state. The torque is low for the supercritical basic flow and increases with the number of vortices.

The behaviour of the flow in the supercritical regime is shown in Figure 9 for the Mode IV with four vortices. The size of the vortices increases with increasing Reynolds number.

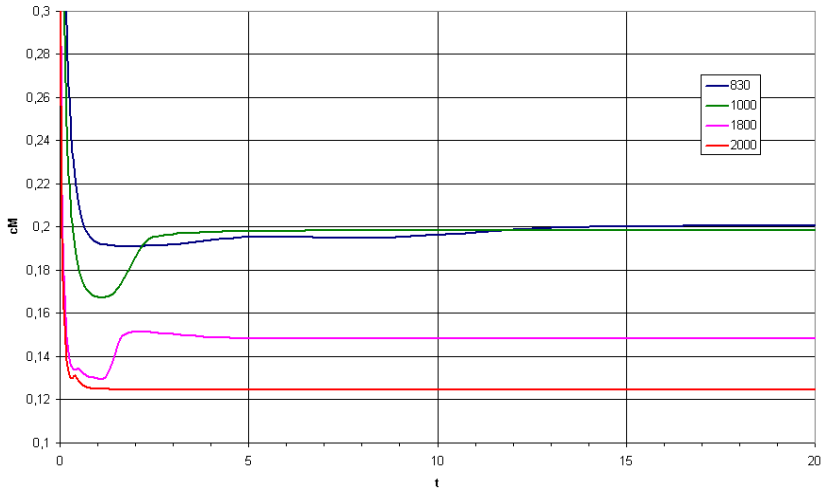

Figure 8. Torque behaviour during the development of the different modes as function of time

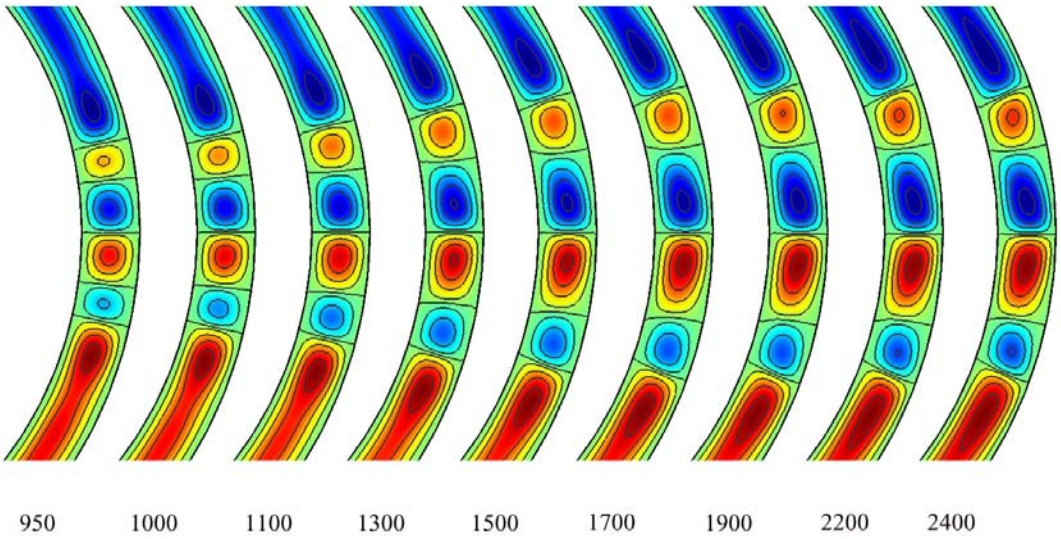

Figure 9. Steady states of the Mode IV with four vortices at different supercritical Reynolds numbers

4. Comparison between numerical and experimental results

With the numerical simulations the non-uniqueness of the supercritical solutions observed in the experiments can be realized. In Figure 10 we see a comparison of the flow structure for the supercritical Mode I without vortices. The experimental result is on the left and the corresponding numerical result on the right in Figure 10.

The Mode III with two vortices is shown in Figure 11. The distance between two arrows on the sphere in the left part of the Figure 11 is proportional to the gap width. The flow is directed towards the equatorial plane in both vortices below and above the equator. The right part shows the corresponding numerical result. The Mode IV with four vortices is shown in Figure 12. It can be seen that the two vortices near the equator are larger than the gap with given by the distance between the two red arrows. The two smaller vortices are rotating in opposite direction of the basic flow. There is a good agreement for the global flow structure between experiment and numerical simulation for all the three symmetric modes.

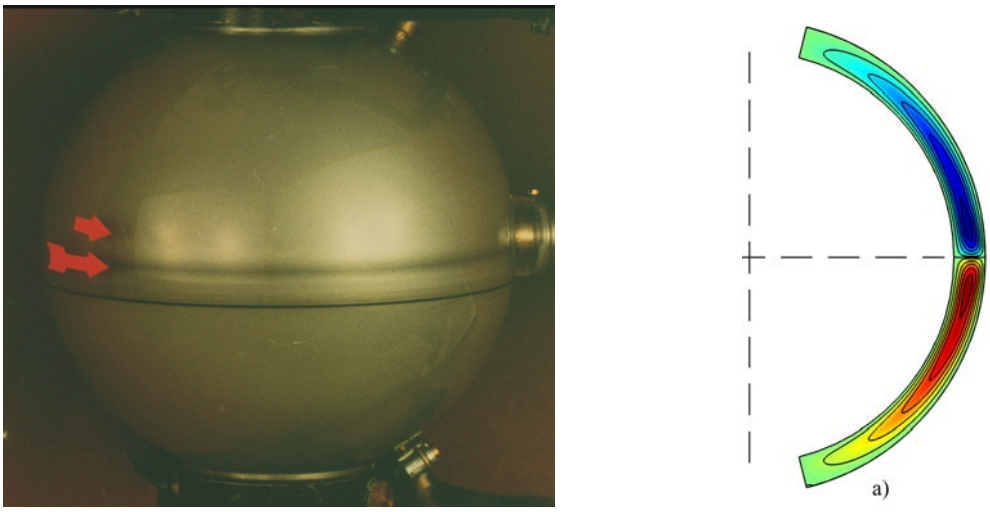

Figure 10. Supercritical Mode I at Re=2600, Comparison of experiment and numerical simulation

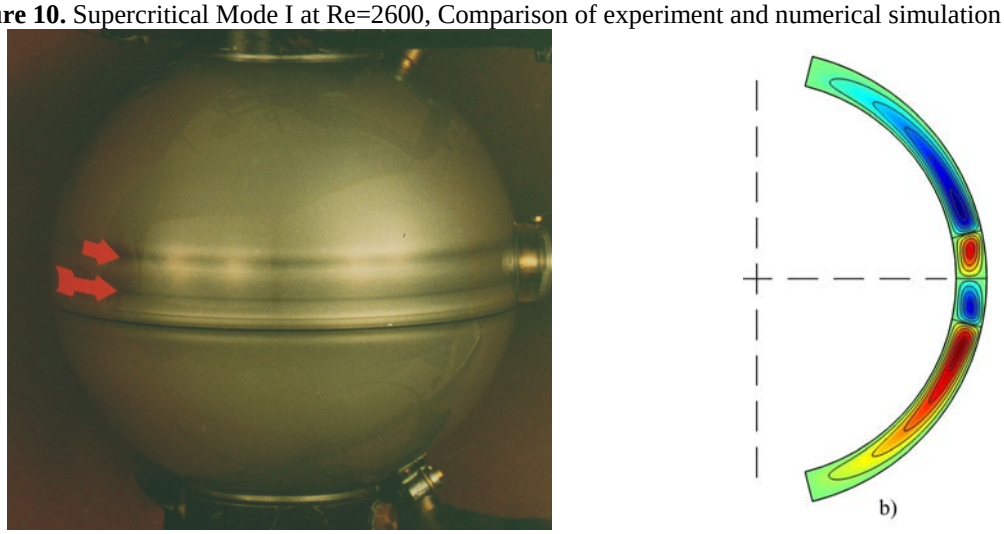

Figure 11. Supercritical Mode III at Re=2600, Comparison of experiment and numerical simulation

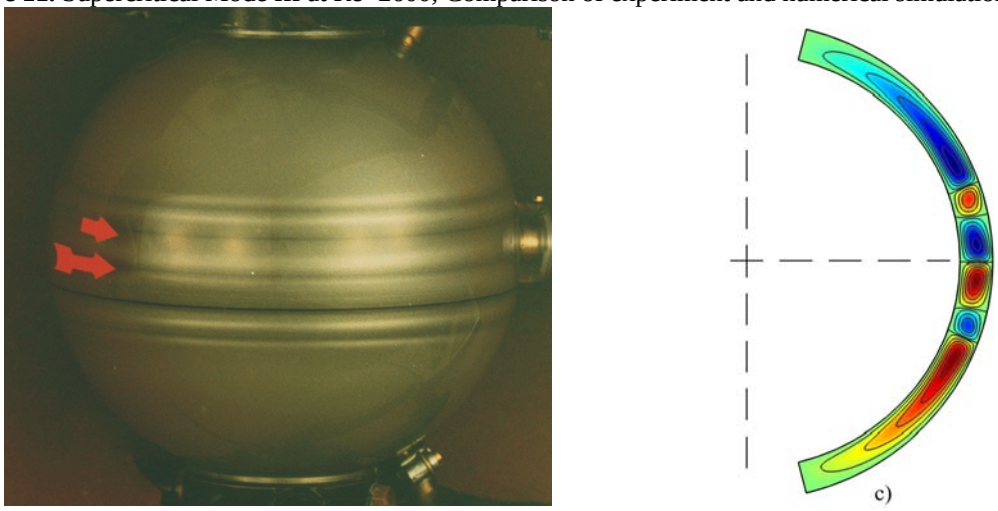

Figure 12. Supercritical Mode IV at Re=2600, Comparison of experiment and numerical simulation

5. Conclusion

This study shows the advantage of COMSOL Multiphysics to simulate spherical gap flows with the swirl flow mode. The non-uniqueness of the supercritical solutions is explored and new routes into the supercritical modes of flow could be found compared to the former simulations with a finite difference method. Further investigations should explore more details of the existence ranges and transitions depending on the Reynolds number and gap geometry.
Other applications in rotating fluids [4,5] show the advantage of this method to investigate rotating fluids with spherical geometries.

6. References

[1] Sawatzki O., Zierep J.: Das Stromfeld im Spalt zwischen zwei rotierenden Kugelflächen, von denen die innere rotiert. Acta Mechanica 9, 13-35 (1970)
[2] Wimmer M.: Experiments on a viscous fluid flow between concentric rotating spheres. J. Fluid Mech. 78, 317-335 (1976)
[3] Bühler K.: *Strömungsmechanische Instabilitäten zäher Medien im Kugelspalt. Habilitationsschrift, Fakultät für Maschinenbau, Universität Karlsruhe 1985*
Fortschritt-Berichte VDI Reihe 7, Nr. 96, Düsseldorf 1985
[4] Bühler K.: Symmetric and asymmetric Taylor vortex flow in spherical gaps. Acta Mechanica 81, 3-38 (1990)
[5] Bühler K., Louw J.W.: Numerical Simulation of the Secondary Flow due to the Coaxial Rotation of two Spheres. Proceedings of the European COMSOL Conference 2007 in Grenoble, France Ed.:J.-M. Petit and O. Squalli, Vol.1 p.326-332
[6] Bühler K., Louw J.W.:*Visualization and Numerical Simulation of the Secondary Flow due to the Coaxial Rotation of two Spheres, International Symposium on Flow Visualization 2008, Nice, France Ed.:J.P. Prenel and Y. Bailly, CD Rom Proceedings Paper 309*

7. Appendix

Table 1: Dimensional Parameters

R_1	Radius of the inner sphere
R_2	Radiusof the outer sphere
$s=R_2-R_1$	Gap width
r	Coordinate in radial direction
z	Coordinate in vertical direction
φ	Circumferential angle
u	Radial velocity
v	Axial velocity
w	Circumferential velocity
t	Time
ϑ_0	Angle at the poles
Ψ	Stream function
ν	Kinematic viscosity

Table 2: Non-dimensional Parameters

$\sigma=s/R_1$	Gap geometry parameter
$Re = \omega \cdot R_1^2/\nu$	Reynolds number